ARTICLE

Fouling-release Property of Water-filled Porous Elastomers

Lai-yong Xie[a,b*], Fei Hong[a,b], Chuan-xin He[b*], Jian-hong Liu[b], Chi Wu[a,c]

a. Hefei National Laboratory for Physical Sciences at Microscale, Department of Chemical Physics, University of Science and Technology of China, Hefei 230026, China
b. School of Chemistry and Chemical Engineering, Shenzhen University, Shenzhen 518060, China
c. Department of Chemistry, The Chinese University of Hong Kong, Hong Kong

(Dated: Received on February 20, 2012; Accepted on February 23, 2012)

Since the fouling-releasing ability of silicone elastomers increases as their modulus decreases, we designed and prepared composites with embedded tiny NaCl crytals that are soluble after their immersion in water, resulting in water-filled porous elastomers. The scanning electron microscope images confirmed such a designed water-filling porous structure. The existence of many micro-drops of water in these specially designed elastomers decreases their shear storage modulus and increases their loss factors. The decrease of shear modulus plays a leading role here and is directly related to a lower critical peeling-off stress of a pseudo-barnacle on them. Therefore, such a novel preparation with cheap salts instead of an expensive silicone provides a better way to make fouling-release paints with a lower modulus, a lower critical peeling-off stress and a better fouling-release property without a significant decrease of their cross-linking density.

Key words: Fouling-release, Porous silicone elastomer, Soluble salt, Pseudo-barnacle adhesion, NaCl, Micro-drop of water

I. INTRODUCTION

Biofouling costs billions of dollars each year in shipping industry because it leads to a higher frictional resistance, a more dry-docking time, bio-corrosion, and an invasion of alien aquatic species [1]. For reducing, if not preventing these effects, antifouling coatings have to be used on ship hulls. Toxic antifouling paints containing copper and other biocides are widely used nowadays and provide an effective control of many biofouling species [2, 3]. However, due to an increasing environmental concern, some of non-toxic approaches have recently been designed and studied to control biofouling. The environment-friendly "biofouling-release coatings" are mainly based on silicone elastomers and become successful replacements in certain areas [1].

It has been suggested that these silicone elastomers control the biofouling by minimizing the adhesion strength between the coating and the organism so that those attached biofouling species are removed by the hydrodynamic peeling force generated from ship movements. In the Kendall's model, the critical adhesion force f of a rigid cylindrical punch on a soft material is used to analyze the fouling-release behavior [4]. The critical adhesion force can be evaluated as a function of the radius of the punch used r, the coating thickness h, the Young's modulus E, the Poisson's ratio v, the surface energy γ, and the bulk modulus K as follows,

$$f = \left(\frac{8\pi r^3 \gamma E}{1-v^2}\right)^{1/2}, \qquad r \ll h \tag{1}$$

$$f = \pi r^2 \left(\frac{2\gamma K}{h}\right)^{1/2}, \qquad r \gg h \tag{2}$$

$$K = \frac{E}{3(1-2v)}$$

Eqs. (1) and (2) show that the adhesion force depends on both the surface energy and modulus. For a thin coating ($r \gg h$), the adhesion force is inversely proportional to the root of the coating thickness. The linkage between the adhesion force and modulus has been confirmed by many previous studies on releasing pseudo-barnacles or barnacles from different silicone elastomers [5−12]. It has been known that the release of a biofouling species from a coating with a lower elastic modulus is normally quicker and easier [13]. The interfacial slippage and friction also play a role in the fouling-release property [14, 15]. However, for a given silicone elastomer, the problem is how to lower its elastic modulus but at the same time maintain its mechanical strength.

It has been known that silicone elastomers have a good fouling-release property because of their low surface energy and low modulus [16−19]. A lot of copolymers which contain PDMS segments were also used to study the fouling-release property [20, 21]. Commercially available "fouling-release coatings" made of sili-

*Authors to whom correspondence should be addressed. E-mail: xiely@mail.ustc.edu.cn, Hcx2002@mail.ustc.edu.cn

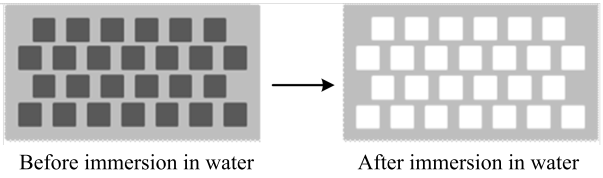

FIG. 1 Schematic process of how water-filled porous elastomers are formed, where small black and white squares represent tiny NaCl crystals and water-filled holes after dissolution and diffusion-out of NaCl, respectively.

cone elastomers have gradually entered market. However, they are generally expensive because of raw materials and require a comparatively high critical navigational speed to remove these attached biofouling organisms [13, 22].

In this work, we adopted a novel approach, namely, uniformly dispersing some cheap tiny salt crystals (*e.g.*, NaCl) into a silicone elastomer with a properly chosen dispersing agent. After painting and curing, a silicone coated with uniformly dispersed tiny salt crystals is formed. The dissolution and diffusion-out of tiny salt crystals lead to many small water-filled micro-pores after its immersion in water, resulting in a painting with a much lower modulus in comparison with those without any loaded salts. Figure 1 schematically shows such a design. Using this method, we are able to prepare silicone elastomers with a much lower modulus but a similar cross-linking density. Note that using cheap soluble salts to replace part of expensive silicone also reduce the total cost of such fouling-release coatings.

II. MATERIALS AND METHODS

A. Reagents and panel preparation

Xylenes, *n*-octane, sodium chloride were purchased from Alfa Corporation. T-4 RTV silicone rubber base (T-4 base) and curing agent (T-4 curing agent), silane coupling agent KH-570, epoxy E-51, amine-terminated polyether D 230, and dispersant DISPERBYK®-110 were kindly provided by the Dow Corning Co., Ltd., Jiang Su Chenguang Coincident Dose Co., Baling Petrochemical Co., BASF, and BYK Additives & Instruments Co., respectively. All the reagents were used as received without further purification.

Model coatings were prepared as follows. T-4 base and dispersant (DISPERBYK®-110) were added into a solvent (a mixture of xylene and n-octane, 65:35 by weight). The mixture was stirred until it became uniform. Such a formed mixture and salt (NaCl) were placed in a stainless steel milling tank (500 mL) containing two different steel balls: 150 and 250 g, respectively, with diameters of 10 and 5 mm. Large NaCl particles was grinded into tiny crystals and dispersed into T-4 base using a planetary ball mill (QM-1SP2, Nanjing University Instrument Plant) at a milling speed of 450 r/min for 2 h.

TABLE I Compositions of different coatings (silicone elastomers), where a mixture of xylene and *n*-octane (65:35, mass ratio) was used as solvent (65 g).

Coating	1	2	3	4	5
T-4 base/g	40	40	40	40	23.7
NaCl/g	0	40	40	40	40
DISPERBYK®-110/g	0	2	4.4	7.43	4.4
T-4 curing agent/g	4	4	4	4	2.37

Table I summarizes compositions of different samples used in this work. The final coatings used hereafter were prepared by mixing grinded mixture and T-4 curing agent. After stirring for 20 min, the mixture was applied to a glass microscope slide and a glass panel (8 cm×8 cm), respectively. The glass slide and panel were pre-treated by KH-570 to enhance their adhesion to the coatings. Each coating was finally dried first at room temperature for 48 h, then at 60 °C for 4 h and further at 100 °C for 12 h. The thicknesses of these dried coatings were controlled to be ∼500 μm.

B. Surface energy evaluation and SEM measurement

The surface energy γ of each coating was evaluated using two liquid probes (water and *n*-hexadecane) with the Owens-Wendt-Rable-Kaeble (OWRK) model:

$$\gamma_{\rm s} = \gamma_{\rm s}^{\rm d} + \gamma_{\rm s}^{\rm p} \quad (3)$$

$$\gamma_{\rm l} = \gamma_{\rm l}^{\rm d} + \gamma_{\rm l}^{\rm p} \quad (4)$$

$$\gamma_{\rm l}(1+\cos\theta) = 2(\gamma_{\rm s}^{\rm d}\gamma_{\rm l}^{\rm d})^{1/2} + 2(\gamma_{\rm s}^{\rm p}\gamma_{\rm l}^{\rm p})^{1/2} \quad (5)$$

where the subscripts "l" and "s" denote liquid and solid, respectively; the superscripts "d" and "p" denote the corresponding dispersive and polar components, respectively; and θ is the contact angle [23]. Therefore, after measuring contact angles of two liquids with known $\gamma_{\rm l}^{\rm d}$ and $\gamma_{\rm l}^{\rm p}$ on a coating, one can calculate its $\gamma_{\rm s}$ on the basis of Eqs. (3)−(5).

After immersing the slide with a testing coating in water for different times, we rinsed the coating surface several times with distilled water and then gently dried it with tissue. Further, we purged the coating by nitrogen for 30 s at room temperature before measuring the contact angle using a Powereach JC2000C Optical Contact Angle Meter with Milli-Q water and *n*-hexadecane at 20 °C, respectively. In each contact-angle measurement, one little drop of water was formed on the tip of a micro-pipette by controlling a manual liquid dispenser. After the coating on the glass slide is raised to contact the drop, we lowered the glass slide to detach the drop from the micro-pipette. The contact angle was imaged and recorded. For each given liquid, three different points on each coating were measured. Their averaged value was used to calculate $\gamma_{\rm s}$ of each coating by Eqs. (3)−(5).

DOI:10.1088/1674-0068/25/03/330-334

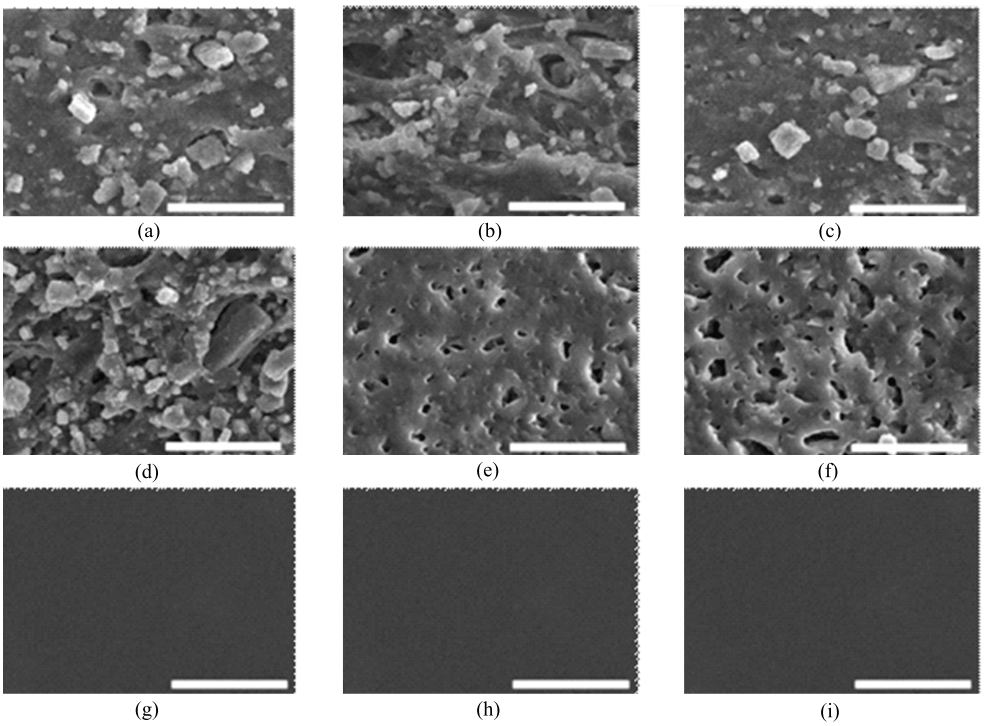

FIG. 2 SEM images of different coatings, where (a), (b), (c), (d), are respectively the cross-sections of coatings 2, 3, 4, and 5 before their immersion in water; (e) and (f) are respectively the cross-sections of coatings 4 and 5 after their immersion in water for 70 h; and (g), (h), and (i) are respectively the surfaces of coating 1, 4, and 5 after their immersion in water for 70 h. The white scale is 20 μm.

For the morphological study of these coating made of silicone elastomers with embedded tiny NaCl crystals, each slide with a coating was first immersed in water for 70 h and then rinsed with distilled water and dried at room temperature for 24 h as previously described before they were imaged by a Hitachi S-3400 scanning electron microscope (SEM). Both the cross-sections of the coatings before and after its immersion in water were measured.

C. Rheological measurement

Each coating was peeled off from the slide and cut into small discs (8 mm in diameter). They were immersed in distilled water for different time periods before being taken out to measure its immersing time dependent thickness. The loss factor and shear storage modulus were measured by a TA AR1000 Rheometer with 8-mm Parallel plates at 20 °C. The torsion oscillating measurement model was chosen with a strain of 2.5×10^{-3}, a frequency of 1 Hz and an initial normal force of 5 N.

D. Pseudo-barnacle adhesion test

The pseudo-barnacle adhesion measurement was performed according to ASTM D5618 [24]. After immersing in water for 70 h, each panel with a coating was pulled out and its coating surface was gently washed with distilled water, dried with tissue and then purged by nitrogen at room temperature for 30 s. A cylindrical aluminum stud (1 cm in diameter and 1 cm in height) was glued to the coating surface with a adhesive mixture of equivalent amounts of E-51 and D230. These panels, each with an adhered stud, were placed inside an enclosed box with a thin layer of water in its bottom to prevent the evaporation of the micro-drops of water in the coating during the curing process. The curing was processed for 7 days at room temperature to harden the adhesive before the peeling test. The Shimpo FGJ-20 force gauge was bound to a traveling rack, moving at 0.9 mm/s parallel to the coating surface. Five pseudo-barnacles adhesion measurements were done for each sample.

III. RESULTS AND DISCUSSION

Figure 2 (a)−(d) clearly show that tiny NaCl crystals were well dispersed in these coatings. After their immersion in water, the dissolution and diffusion-out of these NaCl crystals leave many small holes in these silicone elastomers to make them porous, as shown in Fig.2 (e) and (f). From Fig.2 (g)−(i), we can see the surfaces of coating 1, 4, and 5 are all smooth after immersion. On the other hand, Fig.3 shows that the surface energies of different coatings before and after their immer-

DOI:10.1088/1674-0068/25/03/330-334

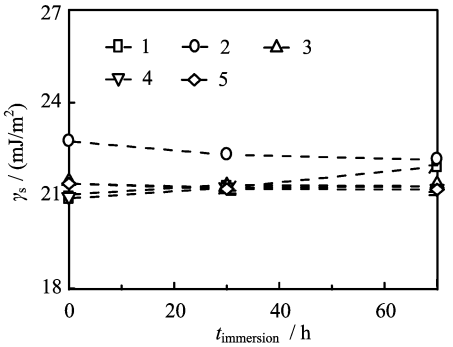

FIG. 3 Time dependence of γ_s of coatings 1−5 after their immersion in water, γ_s was determined by Eqs. (3) and (4).

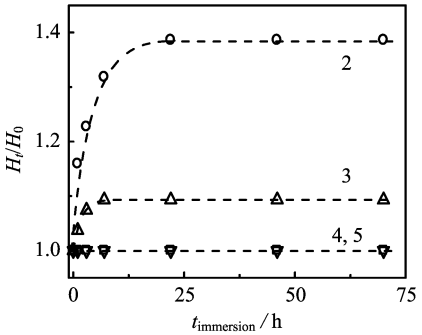

FIG. 4 Immersion-time dependence of thickness change of Coatings 2−5 in water. H_0 and H_t are thicknesses of each coating before and after its immersion in water after different hours.

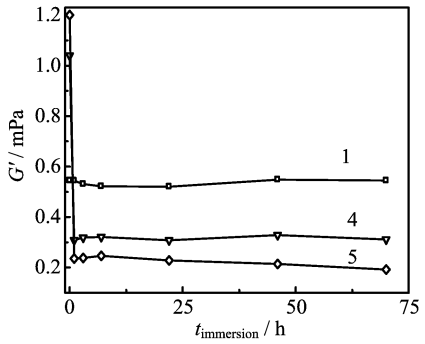

FIG. 5 Immersion-time dependence of storage modulus of different coatings after they are immersed in water.

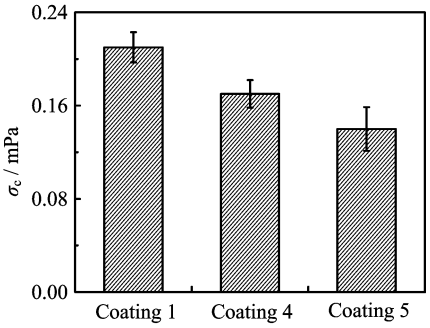

FIG. 6 Effect of salt loading on critical stress (σ_c) of peeling pseudobarnacle off from coating (*i.e.*, adhesion strength), tests were done after their immersion in water for 70 h.

sion in water are similar, independent of the immersion time. These are presumably due to the preferential distribution of hydrophobic silicone chains on the coating surface during the coating curing process, minimizing the surface energy and keeping tiny NaCl crystals away from surface.

Figure 4 shows that after immersed in water, for coatings 4 and 5, there is no change in the coating thicknesses, while for coatings 2 and 3, they become thicker. Relatively, coating 2 has a larger change in its relative thickness and a slightly slower swelling kinetics than coating 3. Such differences can be attributed to difference in these compositions ratios of dispersant DISPERBYK®-110 to T-4 base. Namely, some of tiny NaCl crystals are trapped inside so that their dissolution is hindered, resulting in a salt concentration difference between inside and outside of the coating. Therefore, the osmotic pressure difference drives more water into the coating, leading to its swelling until the osmotic pressure is balanced by the elastic pressure generated inside a swollen gel network. It should be stated that the dispersant is a copolymer with anionic acidic groups. Besides covering the surface of tiny NaCl crystals, the dispersant also form some micro-phases inside the coatings because it is incompatible with T-4 base. As expected, adding more dispersant copolymer chains results in more micro-phases that potentially interlink from each other to form channels for quicker dissolution and diffusion-out of NaCl after the coatings are immersed in water. For coatings 4 and 5, the dissolving and diffusing-out of NaCl are so fast that no obvious thickness change was observed.

Figure 5 shows that the shear storage modulus G' quickly decreases and approaches a constant ∼1 h after each coating is immersed into water. It is clear that the coatings loaded with more tiny NaCl crystals have a lower G' because the dissolution and diffusion-out of NaCl lead to more small holes filled with water. Previously, a pseudo-barnacle adhesion testing method was developed by Swain *et al.*, which correlates well with barnacle adhesion in an open sea [24]. Therefore, the pseudo-barnacle adhesion strength was measured instead of real barnacle adhesion strength for silicone coatings to evaluate their fouling-release abilities. Note that coatings 2 and 3 were improper for the pseudo-barnacle adhesion test because they were detached from the glass substrate or deformed by the stress generated between the highly swollen coating and the glass substrate, which means that the compositions are not good.

Figure 6 shows that coatings 4 and 5 have better fouling-release ability than that with no salt (coating 1) and the fouling-release ability becomes better as more NaCl crystals are loaded into the coating, presumably

DOI:10.1088/1674-0068/25/03/330-334

TABLE II Properties of different coatings after their immersion in water for 70 h.

Sample	G'/MPa	σ_c/MPa	tanδ	(G_a/h)/MPa
Coating 1	0.545	0.21	0.073	0.040
Coating 4	0.311	0.17	0.089	0.046
Coating 5	0.192	0.14	0.113	0.051

because those water-filled small holes in the elastomers reduce its modulus, which actually proves our designing concept. Further, we can calculate the fracture energy, defined as G_a/h, where h is the coating thickness, from σ_c and G' by the following equation [9].

$$\sigma_c = \sqrt{\frac{2G'G_a}{h}} \tag{6}$$

Any difference in G_a among different coatings should be attributed to dissipative process since their surface energy and thickness are similar.

Table II shows that coatings with loaded tiny NaCl crystals have a higher tanδ, a lower G', and a lower δ_c than that with no salt. The correlation between G_a/h and tanδ is excellent where the correlation coefficient R is 0.953 and p of test of significance is 0.019. Therefore, those water-filled small holes in these elastomers indeed increase the dissipative energy (tanδ) and the fracture energy, adversely affects the release of pseudo-barnacle. On the other hand, they also decrease G', which decreases the peeling-off stress based on Eq.(6). For our coatings, the decrease of G' plays a leading and dominant role so that their critical peeling-off stress decreases when more water-filled holes are generated. Therefore, using tiny NaCl crystals as fillers can facilely and cheaply prepare porous silicone elastomers with better fouling-release ability.

IV. CONCLUSION

Loading tiny NaCl crystals into fouling-release coatings made of silicone elastomers with the help of a properly chosen dispersant can lead to porous coatings with many tiny water-filled holes because of dissolution and diffusion-out of salt after they are immersed into water. The existence of these tiny water-filling holes in elastomers decreases their storage modulus G' and increases tanδ. G' and tanδ have opposite effects on the critical stress of peeling a pseudo-barnacle off their surface. Our results reveal that the decrease of G' plays a leading and dominant role here so that their critical peeling-off stress decreases as more salts are added into silicone elastomers, making them better fouling-release coatings. The current study proves our designing concept and demonstrates a facile and cheaper method to make fouling-release coatings better without a significant decrease of their cross-linking density.

V. ACKNOWLEDGMENTS

This work was supported by the National Natural Science Foundation of China (No.20934005, No.21004040, No.51173177), National High Technology Research and Development Program of China (No.2009AA03Z513), the Natural Science Foundation of SZU (No.201102), and Hong Kong Special Administration Region Earmarked (RGC) Projects (CUHK4039/08P, No.2160361; CUHK4042/09P, No.2160396; CUHK4042/10P, No.2130241; No.2060405).

[1] L. D. Chambers, K. R. Stokes, F. C. Walsh, and R. J. K. Wood, Surf. Coat. Tech. **201**, 3642 (2006).
[2] D. M. Yebra, S. Kiil, and K. Dam-Johansen, Prog. Org. Coat. **50**, 75 (2004).
[3] E. Almeida, T. C. Diamantino, and O. D. Sousa, Prog. Org. Coat. **59**, 2 (2007).
[4] K. Kendall, J. Phys. D **4**, 1186 (1971).
[5] J. G. Kohl and I. L. Singer, Prog. Org. Coat. **36**, 15 (1999).
[6] R. F. Brady and I. L. Singer, Biofouling **15**, 73 (2000).
[7] I. L. Singer, J. G. Kohl, and M. Patterson, Biofouling **16**, 301 (2000).
[8] M. Berglin, N. Lönn, and P. Gatenholm, Biofouling **19**, 63 (2003).
[9] J. Stein, K. Truby, C. Darkangelo-Wood, M. Takemori, M. Vallanve, G. Swain, C. Kavanagh, B. Kovach, M. Schultz, D. Wiebe, E. Holm, J. Montemarano, D. Wendt, C. Smith, and A. Meyer, Biofouling **19**, 87 (2003).
[10] Y. Sun, S. Guo, G. C. Walker, C. J. Kavanagh, and G. W. Swain, Biofouling **20**, 279 (2004).
[11] D. E. Wendt, G. L. Kowalke, J. Kim, and I. L. Singer, Biofouling **22**, 1 (2006).
[12] J. Kim, B. J. Chisholm, and J. Bahr, Biofouling **23**, 113 (2007).
[13] R. F. Brady, Prog. Org. Coat. **43**, 188 (2001).
[14] B. M. Newby, M. K. Chaudhury, and H. R. Brown, Science **269**, 407 (1995).
[15] B. M. Newby and M. K. Chaudhury, Langmuir **13**, 1805 (1997).
[16] M. E. Callow and R. L. Fletcher, Int. Biodeterior. Biodegr. **34**, 333 (1994).
[17] R. F. Brady, Chem. Ind. **6**, 219 (1997).
[18] R. F. Brady Jr. and Irwin L Singer, Biofouling **15**, 45 (2000).
[19] C. Anderson, M. Atlar, M. Callow, M. Candries, A. Milne, and R. L. Townsin, J. Marine Des. Oper. Par B4 11 (2003).
[20] J. Fang, A. Kelarakis, D. Y. Wang, E. P. Giannelis, J. A. Finlay, M. E. Callow, and J. A. Callow, Polymer **51**, 2636 (2001).
[21] A. E. Meraa, M. Goodwin, J. K. Pike, and K. J. Wynne, Polymer **40**, 419 (1999).
[22] M. Candries, JPCL **18**, 38 (2001).
[23] D. Owens and R. Wendt, J. Appl. Polym. Sci. **13**, 1741 (1969).
[24] G. W. Swain, M. P. Schultz, J. Griffith, and S. Snyder, *Proc. Emerging. Nonmetallic Materials for the Marine Environment*, Hawaii, 60 (1997).

DOI:10.1088/1674-0068/25/03/330-334